Available online at www.sciencedirect.com
ScienceDirect
Journal of Magnetic Resonance 185 (2007) 264–269
JMR Journal of Magnetic Resonance
www.elsevier.com/locate/jmr

Improved heteronuclear dipolar decoupling sequences for liquid-crystal NMR

Rajendra Singh Thakur [a], Narayanan D. Kurur [b,*], P.K. Madhu [a,*]

[a] Department of Chemical Sciences, Tata Institute of Fundamental Research, Homi Bhabha Road, Colaba, Mumbai 400 005, India
[b] Department of Chemistry, Indian Institute of Technology Delhi, Hauz Khas, New Delhi 110 016, India

Received 30 October 2006; revised 3 January 2007
Available online 10 January 2007

Abstract

Recently we introduced a radiofrequency pulse scheme for heteronuclear dipolar decoupling in solid-state nuclear magnetic resonance under magic-angle spinning [R.S. Thakur, N.D. Kurur, P.K. Madhu, Swept-frequency two-pulse phase modulation for heteronuclear dipolar decoupling in solid-state NMR, Chem. Phys. Lett. 426 (2006) 459–463]. Variants of this sequence, swept-frequency TPPM, employing frequency modulation of different types have been further tested to improve the efficiency of heteronuclear dipolar decoupling. Among these, certain sequences that were found to perform well at lower spinning speeds are demonstrated here on a liquid-crystal sample of MBBA for application in static samples. The new sequences are compared with the standard TPPM and SPINAL schemes and are shown to perform better than them. These modulated schemes perform well at low decoupler radiofrequency power levels and are easy to implement on standard spectrometers.

Keywords: Liquid-crystal NMR; Heteronuclear dipolar decoupling; TPPM; SPINAL; Swept-frequency TPPM

1. Introduction

The liquid-crystal phase is characterised by partial or complete alignment of the molecules along a certain direction. It is associated with certain kind of molecules owing to their structure and such structures constitute a large number of biologically important systems. For example, cell membranes, which are essentially lipid bilayers, are more similar to the liquid-crystal phase than to the liquid or the solid phase. Probing these structures along with their dynamics can yield a great amount of novel information. However, such compounds have various levels of structural organisation with each level having its own relevance. Nuclear magnetic resonance (NMR) can be a candidate of choice for such studies as it can reveal various levels of hierarchy in the structure of such systems, as in the case of proteins. However, being a partially aligned phase, resonances in the NMR spectrum are normally broad because of the incomplete averaging of dipolar couplings. This affects the observation of both ^{1}H and ^{13}C nuclear spins on account of homonuclear and heteronuclear dipolar couplings. Unravelling information from ^{13}C spectra requires efficient heteronuclear dipolar decoupling at lower radiofrequency (RF) powers as RF heating can be deleterious to such systems [1–3]. Details of the use of NMR experiments, especially ^{13}C NMR, to the study of liquid crystals can be found in recent reviews [2,4].

Several heteronuclear dipolar decoupling sequences have been suggested for the study of liquid crystals. These include the conventional continuous-wave (CW) method [5], two-pulse phase modulation (TPPM) [6], two of its variants, namely, small phase angle rapid cycling (SPARC) [7] and small phase incremental alternation (SPINAL) [8], and the DROOPY sequences [9]. Interestingly, the SPINAL method [8], originally conceived for static liquid

* Corresponding authors. Fax: +91 22 2280 4610 (P.K. Madhu).
E-mail addresses: nkurur@chemistry.iitd.ernet.in (N.D. Kurur), madhu@tifr.res.in (P.K. Madhu).

1090-7807/$ - see front matter © 2007 Elsevier Inc. All rights reserved.
doi:10.1016/j.jmr.2007.01.003

crystals, has become routine in magic-angle spinning (MAS) experiments in solid-state NMR.

The SPARC scheme reported by Fung et al. [7] was an improvement over TPPM [6] and SPINAL [8], again from the group of Fung, was an improvement over SPARC. Whilst SPARC relies on rapid phase cycling, SPINAL, in addition, involves phase increments. Such methods generate frequency modulations and an intuitive understanding of the efficiency of such sequences may be obtained on the basis of the Fourier picture of the corresponding RF schemes [8]. Recently, we proposed an alternative heteronuclear dipolar decoupling scheme in which the pulse durations in the standard TPPM scheme were modulated [10]. This was shown to generate a normal distribution of Fourier components compared to SPINAL. The sequence, called SW_f-TPPM, was shown to be robust with respect to various experimental parameters in comparison with both TPPM and SPINAL [11]. Subsequently, we have investigated various other RF modulated schemes for heteronuclear dipolar decoupling arrived at mainly on the basis of the distribution of Fourier components. A detailed report on the design of these schemes is currently under preparation.

In addition to SW_f-TPPM, we here concentrate on two new RF modulated pulse schemes which were found to perform better at lower spinning frequencies for MAS experiments in solid-state NMR. We report in this manuscript the results of applying these sequences for heteronuclear dipolar decoupling in a liquid crystal. These sequences are compared with both TPPM and SPINAL over which they give an improvement in sensitivity and resolution. We also revisit the routinely used SPINAL-64 sequence and find that a systematic optimisation of the initial phase angle leads to considerable improvement in its performance. The new RF modulated schemes are easy to design and implement on modern NMR spectrometers.

2. Experimental

All experiments were performed on a Bruker AV500 MHz spectrometer equipped with a double-resonance BBI probe. The experiments were performed on a liquid-crystal sample of MBBA maintained at 22 °C. The gas flow rate was appropriately regulated (in excess of 11 l/min) to keep the temperature steady. In addition, recycle delays of 40 s were used for a decoupling RF power of 30 kHz and 30 s for power levels of 25 and 20 kHz. The acquisition time was 30 ms for the RF power level of 30 kHz and 40 ms for power levels of 25 and 20 kHz and were chosen to avoid RF heating. For these acquisition times some spectra had truncation artefacts, especially at higher decoupling powers. The values chosen closely follow suggestions of Fung [2].

3. Sequence design, results and discussions

We here compare five decoupling sequences, namely, TPPM, SPINAL, and three modulated TPPM sequences, in which the frequencies are swept, notated as SW_f-TPPM, SW_f^{tan}-TPPM, and SW_f^{inv}-TPPM.

TPPM, notated as $R_\phi R_{-\phi}$, is a sequence of 180° pulses, where R denotes the pulse flip angle with phase ϕ. Experimentally both R and ϕ need to be optimised. SPINAL-8 is obtained from the basic TPPM block by varying the values of ϕ and has the form $Q \equiv R_\phi R_{-\phi}$, $R_{\phi+5}R_{-\phi-5}$, $R_{\phi+10}R_{-\phi-10}$, $R_{\phi+5}R_{-\phi-5}$. SPINAL-64 is of the form $Q\overline{Q}Q\overline{Q}Q\overline{Q}Q\overline{Q}$ with each Q representing SPINAL-8. In the original report ϕ was set to 10° (referred to here as SPINAL-$64_{\phi=10}$) leaving only R to be optimised [8]. We found that allowing ϕ to vary improved the decoupling efficiency of SPINAL-64. We observed that $\phi = 15°$ (referred to here as SPINAL-$64_{\phi=15}$) gave better performance than $\phi = 10°$ for the sample under study. Increasing ϕ beyond 15° was detrimental to the decoupling efficiency.

The design of the swept-TPPM schemes was based on modulating the values of pulse duration (as against ϕ for SPINAL) with respect to a central pulse pair whose duration τ_ϕ could be comparable to the optimum TPPM pulse R. All such schemes can be represented by specifying the pulse widths (τ) of each TPPM pair as phase ϕ is constant. The form of SW_f-TPPM approximates a tangential sweep as three linear segments leading to a sequence of the form [10]: {[$0.78\tau_\phi 0.78\tau_{-\phi}$] [$0.86\tau_\phi 0.86\tau_{-\phi}$] [$0.94\tau_\phi 0.94\tau_{-\phi}$] [$0.96\tau_\phi 0.96\tau_{-\phi}$] [$0.98\tau_\phi 0.98\tau_{-\phi}$] [$\tau_\phi \tau_{-\phi}$] [$1.02\tau_\phi 1.02\tau_{-\phi}$] [$1.04\tau_\phi 1.04\tau_{-\phi}$] [$1.06\tau_\phi 1.06\tau_{-\phi}$] [$1.14\tau_\phi 1.14\tau_{-\phi}$] [$1.22\tau_\phi 1.22\tau_{-\phi}$]}. Here, τ_ϕ and ϕ need to be optimised. The numbers multiplying τ determine the profile of the frequency modulation which we notate as f_i.

SW_f^{tan}-TPPM is a pure tangential sweep where the pulse durations were calculated analytically resulting in a sequence of larger sweep width and of a form: {[$0.65\tau_\phi 0.65\tau_{-\phi}$] [$0.75\tau_\phi 0.75\tau_{-\phi}$] [$0.85\tau_\phi 0.85\tau_{-\phi}$] [$0.90\tau_\phi 0.90\tau_{-\phi}$] [$0.94\tau_\phi 0.94\tau_{-\phi}$] [$0.96\tau_\phi 0.96\tau_{-\phi}$] [$0.98\tau_\phi 0.98\tau_{-\phi}$] [$\tau_\phi \tau_{-\phi}$] [$1.02\tau_\phi 1.02\tau_{-\phi}$] [$1.04\tau_\phi 1.04\tau_{-\phi}$] [$1.06\tau_\phi 1.06\tau_{-\phi}$] [$1.10\tau_\phi 1.10\tau_{-\phi}$] [$1.15\tau_\phi 1.15\tau_{-\phi}$] [$1.25\tau_\phi 1.25\tau_{-\phi}$] [$1.35\tau_\phi 1.35\tau_{-\phi}$]}.

SW_f^{inv}-TPPM was constructed by taking the inverse of the pulse durations that formed a linearly swept SW_f-TPPM sequence where the initial pulse duration was set to $0.5\tau_\phi$ and the final pulse duration was $1.5\tau_\phi$ with each pulse pair incremented by $0.1\tau_\phi$ comprising of again 11 pulse pairs. This mimics, to some extent, the design of the swept fast-amplitude modulated (SW-FAM($1/\tau$)) sequence demonstrated recently for the sensitivity enhancement of static half-integer spin quadrupolar nuclei [13], that resulted in a large sweep width. The sequence so constructed has the form: {[$0.67\tau_\phi 0.67\tau_{-\phi}$] [$0.71\tau_\phi 0.71\tau_{-\phi}$] [$0.77\tau_\phi 0.77\tau_{-\phi}$] [$0.83\tau_\phi 0.83\tau_{-\phi}$] [$0.91\tau_\phi 0.91\tau_{-\phi}$] [$\tau_\phi \tau_{-\phi}$] [$1.11\tau_\phi 1.11\tau_{-\phi}$] [$1.25\tau_\phi 1.25\tau_{-\phi}$] [$1.43\tau_\phi 1.43\tau_{-\phi}$] [$1.67\tau_\phi 1.67\tau_{-\phi}$] [$2.00\tau_\phi 2.00\tau_{-\phi}$]}.

Fig. 1 shows a spectrum of MBBA acquired with $SPINAL_{\phi=10}$, $SPINAL_{\phi=15}$, SW_f-TPPM, SW_f^{tan}-TPPM, and SW_f^{inv}-TPPM decoupling schemes applied on-resonance at an RF power level of 25 kHz. The phase values of the modulated sequences were 35°, 35°, and 45° for

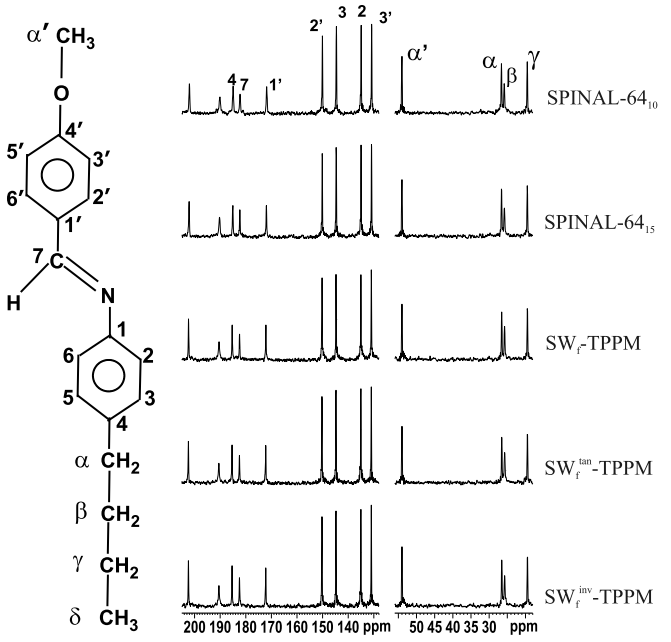

Fig. 1. Spectra of MBBA obtained with the various decoupling schemes SPINAL$_{\phi=10}$, SPINAL$_{\phi=15}$, SW$_f$-TPPM, SW$_f^{tan}$-TPPM, and SW$_f^{inv}$-TPPM applied at on resonance. The structure of MBBA along with peak assignments is also shown.

SW$_f$-TPPM, SW$_f^{tan}$-TPPM, and SW$_f^{inv}$-TPPM sequences, respectively. In general SPINAL$_{\phi=15}$ and the swept-TPPM sequences perform well for all the ^{13}C resonances, and in particular, SW$_f^{tan}$-TPPM and SW$_f^{inv}$-TPPM sequences perform better than the other sequences considering the overall spectral appearance.

One of the reasons for the relatively better performance of the swept-TPPM sequences could be the inherent larger sweep width. This aspect is borne out in Fig. 2 where the time profile (f_i) (top row) and the power spectrum (bottom row) of each of the swept-TPPM sequences are shown.

Heteronuclear dipolar decoupling schemes, besides providing an intensity gain for the resonances, should also be robust with respect to experimental parameters such as the proton off-resonance irradiation, $\Delta\omega(^1H)$, pulse duration, and pulse phase. The schemes should also be spectrometer friendly for routine implementation a fact which TPPM and its variants including the swept-TPPM sequences satisfy.

Fig. 3, left column, shows the spectrum of MBBA acquired with SPINAL$_{\phi=10}$, SPINAL$_{\phi=15}$, SW$_f$-TPPM, SW$_f^{tan}$-TPPM, and SW$_f^{inv}$-TPPM decoupling schemes applied off-resonance by 1 kHz. It may be noted from this plot and Fig. 1 that as the proton off-resonance value increases, the efficiency of the swept-TPPM sequences, in particular the SW$_f^{inv}$-TPPM and SW$_f^{tan}$-TPPM schemes, remains largely unaffected. The robustness to proton offset of these sequences is further illustrated by plotting the intensity of C_7, C_β, and C_α peaks as a function of the ^{1}H off-resonance, $\Delta\omega(^1H)$, for SPINAL$_{\phi=10}$, SPINAL$_{\phi=15}$, SW$_f$-TPPM, SW$_f^{tan}$-TPPM, and SW$_f^{inv}$-TPPM sequences in Fig. 3, right column. The relatively better robust perfor-

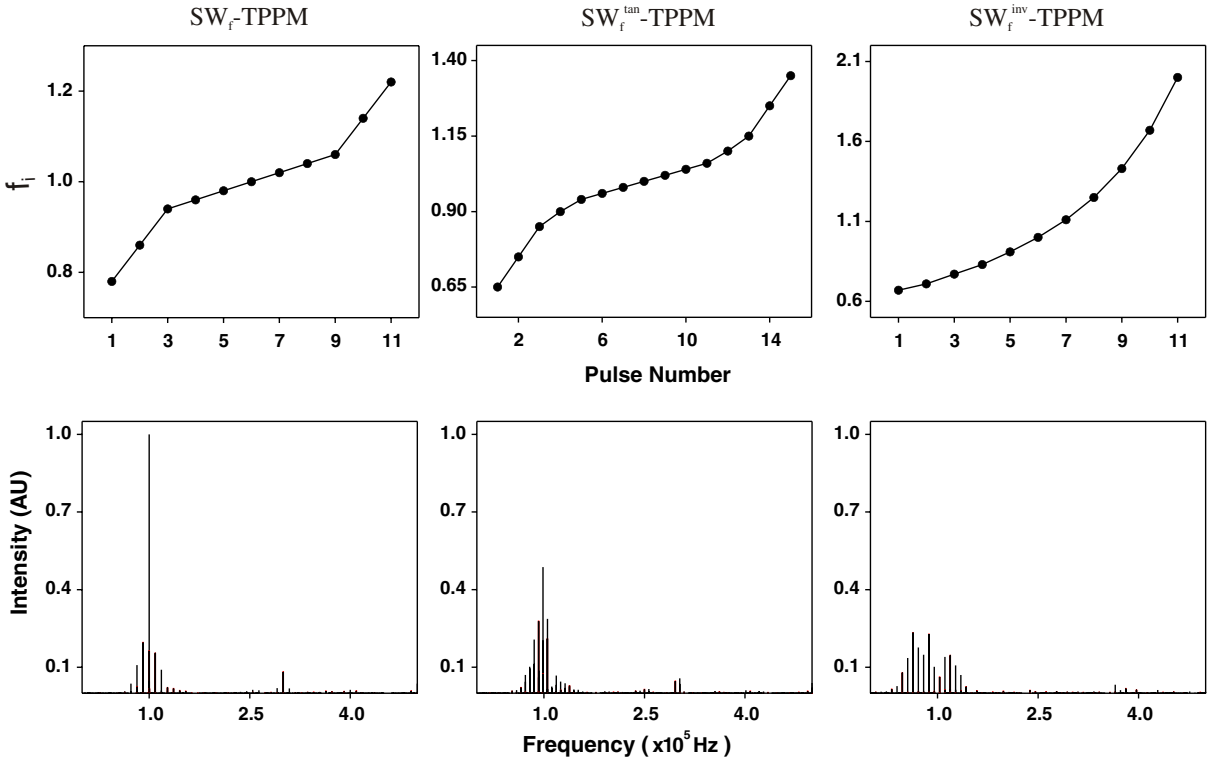

Fig. 2. The time-domain profile (top row) and the power spectrum (bottom row) of SW$_f$-TPPM (left column), SW$_f^{tan}$-TPPM (middle column), and SW$_f^{inv}$-TPPM (right column).

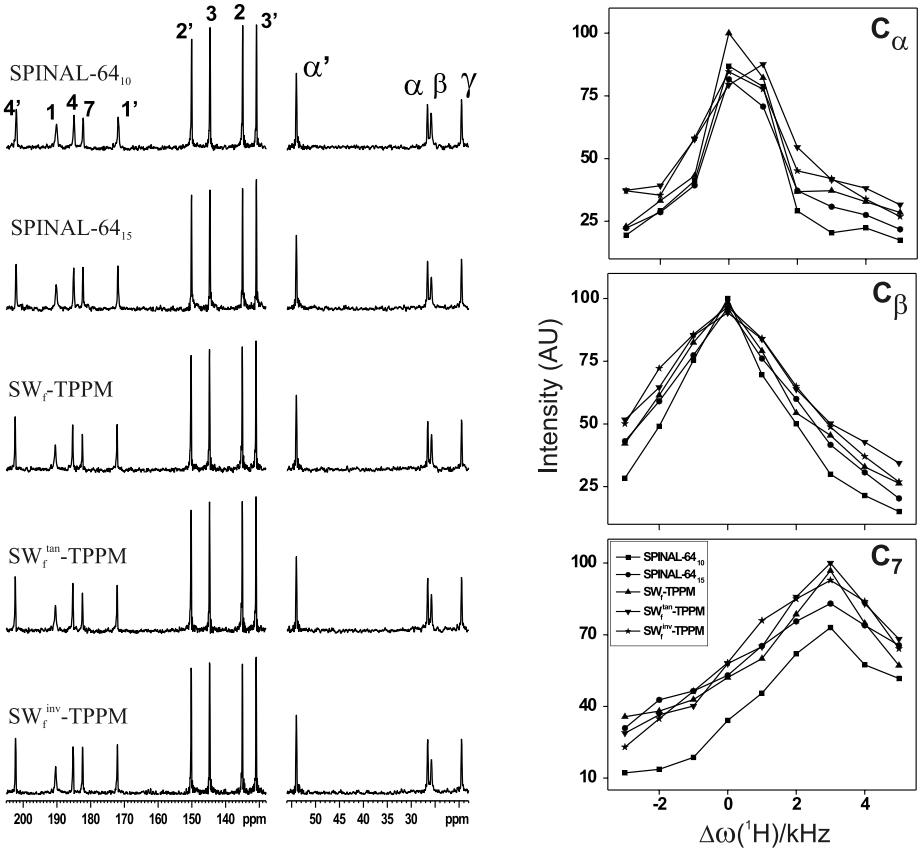

Fig. 3. Left column shows the spectra of MBBA obtained with decoupling schemes SPINAL$_{\phi=10}$, SPINAL$_{\phi=15}$, SW$_f$-TPPM, SW$_f^{tan}$-TPPM, and SW$_f^{inv}$-TPPM applied at off resonance. Right column shows the intensity of the C_α, C_β, and C_7 peaks of MBBA plotted as a function of the $\Delta\omega(^1H)$ for each of the decoupling schemes. Other experimental parameters are mentioned in the text.

mance of the swept-TPPM sequences is clear here with both SW$_f^{tan}$-TPPM and SW$_f^{inv}$-TPPM sequences having a higher band width. Since, the optimum carrier off-set value for each peak is very critical for any decoupling sequence, the relative insensitivity of SW$_f^{tan}$-TPPM and SW$_f^{inv}$-TPPM sequences to $\Delta\omega(^1H)$ is a desirable feature in applications to cover a larger band width uniformly. The RF intensity and the phase values used corresponded to those in Fig. 1. From Figs. 1 and 3 it may be noted that different peaks have different optimum carrier off-set values and off-resonance tolerance is necessary for a better spectrum.

We now investigate the robustness of SW$_f^{tan}$-TPPM and SW$_f^{inv}$-TPPM sequences to the phase ϕ. Fig. 4 shows the intensity of C_α (top row) and C_7 (bottom row) peaks as a function of 2ϕ at three RF intensities of 20, 25, and 30 kHz. It can be ascertained that both the sequences are fairly robust to a phase variation from 35° to 45° a feature not shown by other sequences (data not shown).

To ascertain with which phase, ϕ, the swept-TPPM sequences give good performance and also the spectral intensity performance of various decoupling schemes we monitor, in Fig. 5, the intensity of the C_7 peak of MBBA, which is particularly dependent on decoupling efficiency. In each trace the spectrum obtained with TPPM, SPINAL$_{\phi=10}$, SPINAL$_{\phi=15}$, SW$_f$-TPPM, SW$_f^{tan}$-TPPM, and SW$_f^{inv}$-TPPM is shown from left to right. The left, middle, and right columns correspond to decoupling RF powers of 20, 25, and 30 kHz, respectively. The top row corresponds to decoupling with phases optimised for each sequence independently. Table 1 gives the phase values that yielded for each of the sequences the spectra shown in Fig. 5. At all RF power levels SPINAL$_{\phi=15}$ is more efficient than the originaly reported SPINAL$_{\phi=10}$. The performance of SW$_f$-TPPM, SW$_f^{tan}$-TPPM, and SW$_f^{inv}$-TPPM schemes re nearly the same with SW$_f^{inv}$-TPPM having a slight edge over the others which improves at higher RF power levels.

It may be noted from Table 1 that for the swept-TPPM schemes the optimal phase values differ for various RF power levels, the spectra of which are shown in Fig. 5, top row. This is not a desirable condition for a ''black box'' implementation of these schemes. Hence, we have compromised between the conflicting demands of increased sequence optimisation and increased efficiency.

In the first compromisary level, we have used for each sequence the same phase values at all RF power levels but allowed the phase to be different for the different sequences. The results are shown in the middle row of Fig. 5 and the phase values are given in Table 1. Comparison between the top and middle row of Fig. 5 shows that at this level of compromise the changes in the appearance

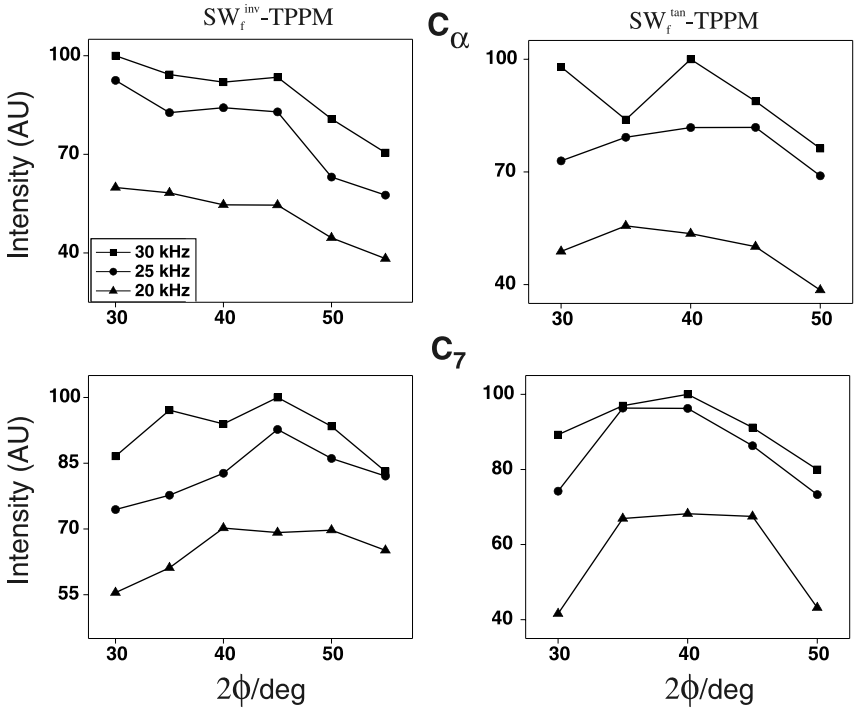

Fig. 4. The intensity of the C_α (top row) and C_7 (bottom row) peaks of MBBA plotted as a function of the phase angle 2ϕ obtained with SW_f^{inv}-TPPM (left column) and SW_f^{tan}-TPPM (right column) sequences for three different RF decoupler power levels of $\omega_1 = 20$, 25, and 30 kHz.

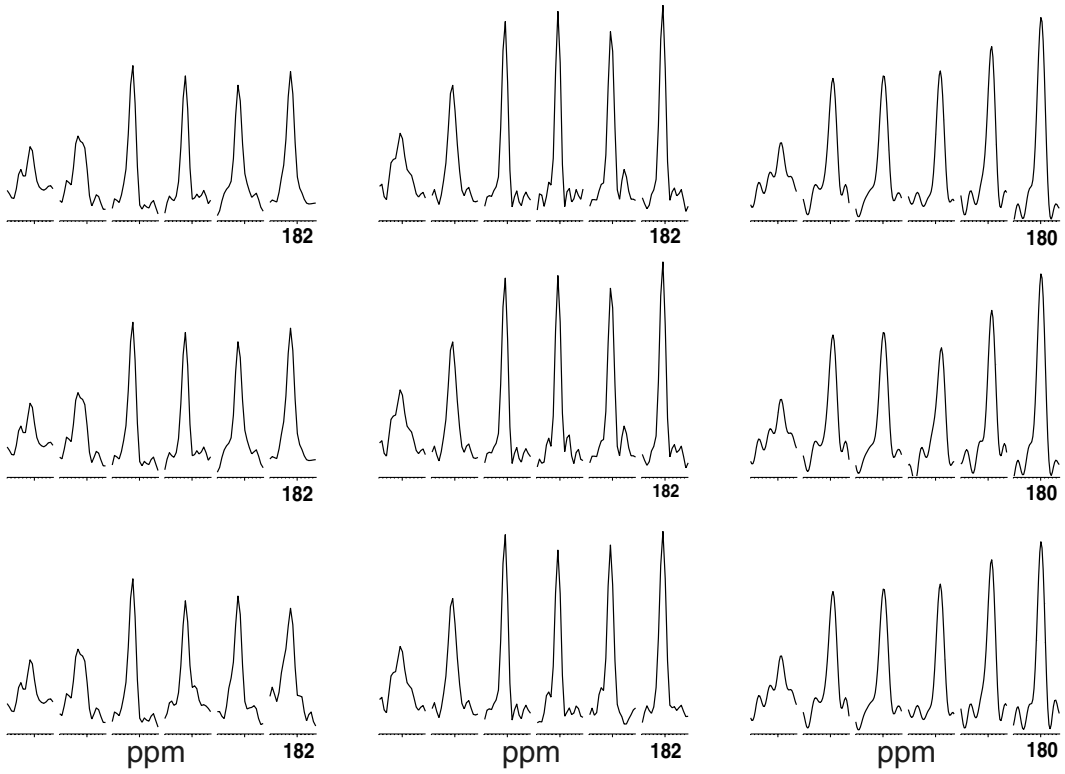

Fig. 5. Spectral intensity comparison of the C_7 peak of MBBA (at ~182 ppm) for the decoupling sequences, TPPM, $SPINAL_{\phi=10}$, $SPINAL_{\phi=15}$, SW_f-TPPM, SW_f^{tan}-TPPM, and SW_f^{inv}-TPPM from left to right, in each trace. The left, middle, and right columns correspond to decoupling RF powers of 20, 25, and 30 kHz, respectively. The top, middle, and bottom rows correspond to decoupling with optimised phases for each sequence at each RF power, with compromise phase values that are different for each of the swept-TPPM sequences but the same for all RF power levels, and compromise phase values that are same for all the swept-TPPM sequences for all RF power levels, respectively. The phase values for each of the decoupling sequences are mentioned in Table 1.

Table 1
Phase values, 2ϕ, for the various decoupling sequences corresponding to the spectra shown in Fig. 5

Decoupling sequence		2ϕ		
		20 kHz	25 kHz	30 kHz
TPPM		25°	30°	25°
SPINAL$_{\phi=10}$		20°	20°	20°
SPINAL$_{\phi=15}$		30°	30°	30°
SW$_f$-TPPM	Top row	35°	30°	40°
	Middle row	35°	35°	35°
	Bottom row	40°	40°	40°
SW$_f^{\tan}$-TPPM	Top row	40°	35°	35°
	Middle row	35°	35°	35°
	Bottom row	40°	40°	40°
SW$_f^{\text{inv}}$-TPPM	Top row	45°	45°	45°
	Middle row	45°	45°	45°
	Bottom row	40°	40°	40°

of the spectrum is hardly discernible, especially at higher powers.

In the second even grosser level of trade-off, the same phase values were used for all the swept-TPPM sequences at all RF power levels. The results are given in the bottom row in Fig. 5 and the phase values can be found in Table 1. The compromise phase values were chosen such that the efficiency drop was not more than 15% from the optimal values. Comparison with the top row shows that a small intensity reduction is perceptible at the lowest RF power of 20 kHz and none at all at the two higher powers.

From the experimental results, in conclusion, for NMR applications in liquid crystals, we recommend the use of either SW$_f^{\tan}$-TPPM or SW$_f^{\text{inv}}$-TPPM scheme as a heteronuclear dipolar decoupling sequence with a compromise phase value of $\phi = 40°$ at any RF power level. The two new sequences, SW$_f^{\tan}$-TPPM and SW$_f^{\text{inv}}$-TPPM, are a subset of a set of decoupling sequences designed by us for use in MAS studies where we observed that the performance of the SW$_f^{\text{inv}}$-TPPM sequence steadily improved as MAS rates were lowered [12]. It suffices to note here that one of the reasons to inspect the efficiency of SW$_f^{\tan}$-TPPM and SW$_f^{\text{inv}}$-TPPM is the greater sweep width inherent in these sequences as evident in Fig. 2.

4. Conclusions

We here revisited the issue of heteronuclear dipolar decoupling in the NMR of liquid crystals. It was found that, for the sample studied, the commonly used SPINAL$_{\phi=10}$, which is better than TPPM, could be replaced with SPINAL$_{\phi=15}$ with improved results for a range of RF decoupling power levels. We have further tested the adaptability of three RF modulated sequences, namely, SW$_f$-TPPM, SW$_f^{\tan}$-TPPM, and SW$_f^{\text{inv}}$-TPPM, that were originally designed for decoupling under MAS, to the study of liquid crystals under static conditions at low RF power levels of 20–30 kHz. These swept-TPPM sequences were selected according to their superior power spectrum profiles in comparison to TPPM and SPINAL. All the swept-TPPM sequences gave nearly the same decoupling efficiency, which was comparable to SPINAL$_{\phi=15}$ and much better than SPINAL$_{\phi=10}$. We emphasise that the phase of all the modulated schemes, including SPINAL, needs to be optimised carefully for the best performance at various RF power levels. The swept-TPPM sequences have a larger band width and are relatively more robust to various experimental parameters. Hence, for the swept-TPPM sequences, a common phase of 40° could be selected with minimal compromise on the decoupling efficiency easing their implementation.

Acknowledgments

P.K.M. acknowledges assistance from Department of Science and Technology, India, under SERC FAST Track Scheme. NDK thanks TIFR for support during a sabbatical stay in which the work was accomplished. We acknowledge Mr. Manoj Naik for technical assistance, and the use of the National Facility for High Field NMR, TIFR, Mumbai.

References

[1] A. Khitrin, B.M. Fung, Design of heteronuclear decoupling sequences for solids, J. Chem. Phys. 112 (2000) 2392–2398.
[2] B.M. Fung, ^{13}C NMR studies of liquid crystals, Prog. NMR Spectrosc. 41 (2002) 171–186.
[3] S.V. Dvinskikh, K. Yamamoto, U.H.N. Dürr, A. Ramamoorthy, Sensitivity and resolution enhancement in solid-state NMR spectroscopy of bicelles, J. Magn. Reson. 184 (2007) 240–247.
[4] S.V. Dvinskikh, D. Sandström, H. Zimmermann, A. Maliniak, Carbon-13 NMR spectroscopy applied to columnar liquid crystals, Prog. NMR Spectrosc. 48 (2006) 85–107.
[5] A.L. Bloom, J.N. Shoolery, Effects of perturbing radiofrequency fields on nuclear spin coupling, Phy. Rev. 97 (1955) 1261–1265.
[6] A.E. Bennett, C.M. Rienstra, M. Auger, K.V. Lakshmi, R.G. Griffin, Heteronuclear decoupling in rotating solids, J. Chem. Phys. 103 (1995) 6951–6958.
[7] Y. Yu, B.M. Fung, An efficient broadband decoupling sequence for liquid crystals, J. Magn. Reson. 130 (1998) 317–320.
[8] B.M. Fung, A.K. Khitrin, K. Ermolaev, An improved broadband decoupling sequence for liquid crystals and solids, J. Magn. Reson. 142 (2000) 97–101.
[9] G. De Paëpe, D. Sakellariou, P. Hodgkinson, S. Hediger, L. Emsley, Heteronuclear decoupling in NMR of liquid crystals using continuous phase modulation, Chem. Phys. Lett. 368 (2003) 511–522.
[10] R.S. Thakur, N.D. Kurur, P.K. Madhu, Swept-frequency two-pulse phase modulation for heteronuclear dipolar decoupling in solid-state NMR, Chem. Phys. Lett. 426 (2006) 459–463.
[11] M. Leskes, R.S. Thakur, P.K. Madhu, N.D. Kurur, S. Vega, A bimodal Floquet description of heteronuclear decoupling in solid-state nuclear magnetic resonance: Adiabatic two-pulse phase modulation sequence, J. Chem. Phys. submitted for publication.
[12] R.S. Thakur, N.D. Kurur, P.K. Madhu, unpublished results.
[13] T. Bräuniger, G. Hempel, P.K. Madhu, Fast amplitude-modulated pulse trains with frequency sweep (SW-FAM) in static NMR of half-integer spin quadrupolar nuclei, J. Magn. Reson. 181 (2006) 68–78.